ELSEVIER

Chemical Engineering Journal 82 (2001) 21–31

Chemical Engineering Journal

www.elsevier.com/locate/cej

Correlation between catalytic activity and support reducibility in the CO_2 reforming of methane over $Pt/Ce_xZr_{1-x}O_2$ catalysts

Fabio B. Noronha[1], Eugene C. Fendley, Ricardo R. Soares[2], Walter E. Alvarez, Daniel E. Resasco*

School of Chemical Engineering and Materials Science, University of Oklahoma, 100 East Boyd Street, Norman, OK 73019, USA

Received 25 May 2000; accepted 24 October 2000

Abstract

We have investigated the relationship between the reducibility of the support and the catalytic activity of supported Pt on a series of catalysts supported on ceria–zirconia mixed oxides. The supports were prepared by co-precipitation with varying Ce/Zr ratios. X-ray diffraction analysis indicated that, depending on the Ce/Zr ratio, solid solutions of cubic $Ce_xZr_{1-x}O_2$ can be formed. The reducibility of the supports was determined by X-ray photoelectron spectroscopy (XPS). After reduction at 773 K in hydrogen the fraction of reduced cerium (i.e. Ce^{3+}) was found to vary with the Ce content, exhibiting a maximum at a composition $Ce_{0.5}Zr_{0.5}O_2$.

A good correlation was found between the reducibility and the catalytic activity. It was found that the conversion of methane and CO_2 obtained on the different catalysts after 22 h on stream went through a maximum as a function of Ce content in the support and that maximum occurred at the composition that exhibited the maximum reducibility. The H_2/CO product ratio was also a function of the support composition, also presenting a maximum for the $Pt/Ce_{0.5}Zr_{0.5}O_2$ catalyst.

The amount and nature of carbonaceous deposits were investigated by combining temperature-programmed oxidation (TPO) studies with (XPS). The TPO profiles of all the spent samples revealed two oxidation peaks, one in the low-temperature region, 623–723 K, and the other in the high-temperature region, 873–973 K. The peak in the high-temperature region is dominant in the unpromoted catalysts, while the peak at low temperature is more prominent in the $Pt/Ce_xZr_{1-x}O_2$ catalysts. XPS exhibits three types of carbon with different binding energies on the spent catalysts, two of them are two forms of coke, and the third one is due to carbonates. However, all of the peaks decreased after an oxidation at intermediate temperatures (i.e. 723 K). Therefore, it appears that the different peaks observed in TPO are not due to different forms of carbon, but rather to different locations on the catalyst surface. The amount of carbonates on the spent catalysts increased with the Ce content, but the correlation between carbonate concentration and activity was not as good as that between reducibility of the support and activity.

Keywords: Catalyst; X-ray photoelectron spectroscopy; Binding energy

1. Introduction

During the last few years, the CO_2 reforming of CH_4 has been intensively investigated for the production of synthesis gas [1–10] as a complementary process of the well-established steam reforming. The possibility of utilizing CH_4 and CO_2 when they are simultaneously present in natural gas reservoirs [11] as well as the H_2/CO product ratio, which is lower than that of steam reforming, make this process attractive for some applications [12]. The primary difficulty associated with the applicability of the CO_2 reforming process is finding a suitable catalyst that will not deactivate under the deactivating conditions needed for this reaction. Since the reforming reaction is highly endothermic, high operating temperatures (∼1073 K) are required to obtain significant conversions. At such high temperatures and in the presence of high concentrations of carbon-containing compounds, the catalyst is susceptible to deactivation, primarily by carbon deposition.

The deposition of carbon in this reaction strongly depends on the type of metal being used. Although, in many reactions Group VIII metals are less prone to coking than Ni, Co, and Fe [7,13], their ability to operate with low carbon deposition under CO_2 reforming of methane is strongly related to their activity for CO_2 dissociation. For example, Ru and Rh are very active for CO_2 dissociation [9] and they have been found able to effect the CO_2 reforming of CH_4

* Corresponding author. Tel.: +1-405-325-4370; fax: +1-405-325-5813.
E-mail address: resasco@ou.edu (D.E. Resasco).
[1] Permanent address: Laboratorio de Catalise, Instituto Nacional de Tecnologia, Av. Venezuela 82, CEP 20081-310 Rio de Janeiro, Brazil.
[2] Permanent address: Universidade Federal de Uberlandia, Av. Joao Naves de Avila 2160, Bloco K, Campus Santa Monica, Uberlandia/MG, Brazil.

1385-8947/01/$ – see front matter
PII: S1385-8947(00)00368-5

in the range 873–1173 K without carbon deposition [5]. Although, the type of support used has been shown to have an effect on the methane reforming activity of metals like Ru or Rh, which are efficient for dissociating CO_2, those effects are much less crucial than in the case of Pt and Pd [14]. This difference is due to the different abilities of the metals for CO_2 dissociation. A metal able to dissociate CO_2 is very efficient in eliminating the carbon produced by the methane decomposition. By contrast, Pt or Pd require the assistance of the support to keep their surface free of carbon. Seshan and co-workers [15,16] first reported that ZrO_2 is a support that promotes stability of Pt, even under severe conditions. Our own investigations, with isotopically labeled molecules, showed that the ZrO_2 support has a strong effect on the activity and stability of the catalyst [17]. In those studies, we found that when the Pt/ZrO_2 catalyst was exposed to pulses of $^{13}CH_4$, formation of ^{13}CO, together with small amounts of $^{13}CO_2$, was observed. X-ray absorption studies demonstrated that the metal particles were in the metallic state. Therefore, the only possible source of oxygen in this experiment was the support. It was then suggested that some of the carbon produced from the decomposition of $^{13}CH_4$ partially reduced the oxide support near the perimeter of the particle. This was a rather unexpected result, since, zirconia is generally considered an unreducible support. However, in agreement with our results other authors have previously reported that a partial reduction of zirconia is possible at high temperatures [18]. The remaining ^{13}C produced from the decomposition of $^{13}CH_4$ was deposited on the Pt metal. Subsequent pulses of $^{12}CO_2$ resulted in the production of both ^{12}CO and ^{13}CO, which supported the idea that carbon was removed from the metal particles under reaction conditions. The results also showed that Pt is needed to catalyze the dissociation of CO_2 since, ZrO_2 alone was not able to do it. Consequently, it was concluded that the dissociation either takes place near the metal–support interface, or it occurs on oxygen vacancies generated during the previous reduction of the support by the methane pulses, which in turn is activated by the metal.

More recently, we have reported that the use of promoters such as cerium oxide improves the activity and stability of Pt/ZrO_2 catalysts under severely deactivating reaction conditions [19–21]. We have interpreted the promoting effects of Ce in terms of a mechanism for the CO_2 reforming on Pt/ZrO_2 catalysts involving two independent paths [16,17,19]. One of them is the decomposition of methane that occurs on the metal, resulting in the formation of hydrogen and carbon, and the other is the reaction of this carbon with oxygen to produce CO. This oxygen can either come from the ZrO_2 support near the metal particle, or from the decomposition of CO_2. In this dual path mechanism, the role of the support is very important. It participates in the dissociative adsorption of CO_2 near the metal particles, transferring oxygen to the coked metal and greatly accelerating the removal of carbon from the metal. Similar results were obtained on $Rh:ZrO_2$ by Efstathiou et al. [22], who demonstrated that the oxygen vacancies in the zirconia support could be replenished by oxygen from the dissociation of CO_2.

Cerium oxide is known to have a very high oxygen exchange capacity [23,24]. This capacity is related to the ability of cerium to reversibly change oxidation states between Ce^{4+} and Ce^{3+} by taking or giving up oxygen [25]. It has been shown [26,27] that the reduction of Ce is not due to a direct release of O_2 to the gas phase, but through a surface reaction with a reductant such as CO, hydrogen, or a hydrocarbon. This reaction is believed to occur at the metal–support interfacial perimeter. Accordingly, the reductant adsorbed on the metal particle would get oxidized at the interface by oxygen from the support [28,29]. Therefore, it is not surprising that the addition of cerium improves the activity of CO_2 reforming catalysts. A second important effect of promoters is the inhibition of Pt particle growth. This effect is not only beneficial for increasing the active metal surface exposed for reaction, but also for maintaining a high metal–support interfacial area, which is crucial for efficient cleaning of the metal particle.

The aim of the present contribution was to evaluate the activity and stability of a series of catalysts: Pt/ZrO_2, Pt/CeO_2, and $Pt/Ce_xZr_{1-x}O_2$ (with $x = 0.25$, 0.50, and 0.75) for the CO_2 reforming reaction and to determine what characteristics of these catalysts affect the activity and stability. We have found that the promotion of the support with cerium depends on the Ce:Zr ratio and it is maximum when this ratio is 1:1. X-ray diffraction (XRD) analysis, X-ray photoelectron spectroscopy (XPS), and temperature-programmed oxidation (TPO) were used to investigate structural properties of the catalysts, the oxidation states of the cerium, zirconium, and platinum, and the coke formation during the reaction, respectively.

2. Experimental

2.1. Catalyst preparation

The ZrO_2 support was prepared by calcination of zirconium hydroxide (Magnesium Electron Inc.—MEI) at 1073 K for 4 h in flowing air. The ceria support was prepared by calcination at 1073 K of CeO_2 obtained from Johnson Matthey. The $Ce_xZr_{1-x}O_2$ supports were synthesized following the method published by Hori et al. [30]. Cerium(IV) ammonium nitrate and zirconium nitrate were dissolved in water, with the appropriate concentrations in order to have the specified Ce/Zr ratios. Then, the ceria and zirconia hydroxides were co-precipitated by increasing the pH through the controlled addition of ammonium hydroxide. After the co-precipitation, the resulting solids were washed with deionized water and calcined at 773 K for 1 h in a muffle. The catalysts were then prepared by incipient wetness impregnation of the supports with an aqueous solution of $H_2PtCl_6 \cdot 6H_2O$. The samples were dried at 393 K

and calcined in a muffle furnace at 673 K, for 2 h. All the catalysts, Pt/ZrO_2, Pt/CeO_2 and $Pt/Ce_xZr_{1-x}O_2$ ($x = 0.25$, 0.50, and 0.75) had the same Pt loading, 1.5 wt.%. The BET surface areas of the supports were determined in a Micromeritics ASAP 2010 adsorption apparatus. As an example of a catalyst on a non-reducible support, an alumina-supported catalyst was prepared using the same Pt loading. The metallic fraction exposed was calculated from pulse hydrogen chemisorption after reduction in hydrogen flow at 773 K and heating in He at 1073 K. The saturation adsorption capacity was obtained at room temperature by sending 20 μl pulses of H_2.

2.2. Catalytic activity

Reactions were performed in a quartz flow reactor with an inner diameter of 0.4 cm and an outer diameter of 0.6 cm. Prior to reaction, 10 mg of catalyst was reduced in situ in H_2 (30 cm^3/min) at 773 K for 1 h and then heated to 1073 K in He (15 cm^3/min). The reactions were performed at 1073 K with a CH_4:CO_2 ratio of 2:1 and a flow rate of 150 cm^3/min. The conditions were chosen to ensure that the reaction was operating far from equilibrium. A ratio of CH_4:CO_2 higher than that at which one would normally operate in a commercial process (e.g. 1:1) was used in order to accelerate the deactivation of the catalyst and make a faster comparison.

The Weisz–Prater criterion for internal diffusion was applied and the results showed that mass transfer limitations were not present in any of the experiments. The exit gases were analyzed using a gas chromatograph (Hewlett Packard HP5890) equipped with a thermal conductivity detector and a Supelco Carboxen 1006 PLOT fused capillary column (30 m, 0.53 mm i.d.), which allowed for separation of H_2, CO, CH_4 and CO_2. The carrier gas used was Ar. Calibration of the GC using varying ratios of the reactants and products resulted in a mole:area ratio for each gas. Quantification of H_2O was not attempted.

2.3. X-ray diffraction and X-ray photoelectron spectroscopy

X-ray diffraction experiments were carried out on a Rigaku Automatic diffractometer (Model D-MAX A) with a curved crystal monochromator and system setting of 40 KV and 30 mA. Data were collected in the angle range 5–70° with a step size of 0.05° and a count time of 1.0 s. The samples were finely ground and then placed on the glass slide using a smear mount technique.

X-ray photoelectron spectroscopy data were recorded on a Physical Electronics PHI 5800 ESCA System with monochromatic Al Kα X-rays (1486.6 eV) operated at 100 W and 15 V in a chamber pressure of approximately 2.0×10^{-9} Torr. A 400 μm spot size and 58.7 eV pass energy were typically used for the analysis. Sample charging during the measurement was compensated by an electron flood gun. The electron takeoff angle was 45° with respect to the sample surface. The reduction or the reaction of the samples was performed in a packed bed micro-reactor with an on/off valve on the top and bottom of the reactor. The reactor with the sample under He was transferred to a glove bag; the sample (in powder form) was placed in a stainless steel holder and it was kept in a vacuum transfer vessel (model 04-110A from Physical Electronics) to avoid any exposure to the atmosphere before the analysis. The XPS data from the regions related to the C (1s), O (1s), Pt (4f), Zr (3d) and Ce (3d) core levels were recorded for each sample. The binding energies were corrected by reference to carbon at 284.8 eV. A non-linear Shirley-type background was used for the area analysis of each peak.

The reducibility of the $Ce_xZr_{1-x}O_2$ supports was evaluated by examination of the fraction of Ce in the 3+ and 4+ oxidation states were through the measurement of the area under a peak at binding energy 916.5 eV, which only contains contribution from the Ce^{4+}, relative to the total area under the Ce (3d) spectrum [31,32]. More details about these calculations are given below.

2.4. Temperature-programmed oxidation (TPO)

TPO experiments were carried out in a micro-reactor coupled to a quadrupole mass spectrometer (MKS, PPT 4.24). The TPO analyses of carbonaceous deposits were used to determine the amount of carbon that was deposited under reaction conditions. After reaction, the samples were cooled to room temperature in He. Then, the samples were heated at a rate of 10 K/min in a 5% O_2:He mixture (30 cm^3/min) up to 1073 K. After the system reached 1073 K, 100 μl of CO_2 pulses were injected in order to calculate the amount of coke formed on the catalysts.

3. Results and discussion

3.1. Characterization of the calcined and reduced catalysts before reaction

Fig. 1 shows the X-ray diffraction patterns obtained on the Pt/ZrO_2, $Pt/Ce_xZr_{1-x}O_2$ catalysts. All the XRD spectra were recorded after calcination at 1073 K. It can be clearly seen that while the monoclinic phase of the zirconia predominated in the Pt/ZrO_2 catalyst, very different patterns were obtained on the Ce-containing supports. We have observed this difference before and indicated that the presence of Ce on the surface of zirconia retards the transformation from tetragonal to monoclinic [33,34]. In fact, in the samples with high Ce content the observed XRD patterns are consistent with the presence of a mixed oxide $Ce_xZr_{1-x}O_2$. In these solids, the Zr is incorporated into the CeO_2 lattice and forms a solid solution with cubic symmetry [35]. It is seen that in the mixed oxides the peak shifts to lower 2θ values from the position corresponding to the tetragonal phase, in agreement with the results reported by Yao et al. [24]. Similarly, Colón et al. [36] have reported that a

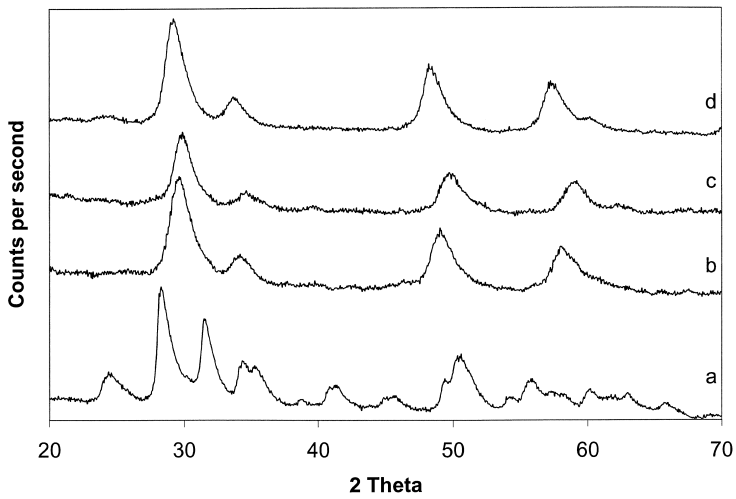

Fig. 1. XRD patterns for the (a) Pt/ZrO_2; (b) $Pt/Ce_{0.25}Zr_{0.75}O_2$; (c) $Pt/Ce_{0.5}Zr_{0.5}O_2$; (d) $Pt/Ce_{0.75}Zr_{0.25}O_2$.

co-precipitation method similar to that used here, results in a $Ce_{1-x}Zr_xO_2$ solid-solution at most compositions with little phase segregation. Although, XRD does not reveal the presence of segregated phases, it is possible that some segregation undetected by XRD may in fact occur. To test this possibility, we have compared the XPS Ce:Zr ratio for the three $Ce_{1-x}Zr_xO_2$ supports. The results are summarized in Table 1. Instead of the linear increase that one could expect for a homogeneous oxide as the Ce:Zr ratio increases, a very high Ce/Zr ratio was observed for the $Ce_{0.75}Zr_{0.25}O_2$ indicating a surface segregation of Ce oxide on this sample. Similarly, the $Ce_{0.25}Zr_{0.75}O_2$ exhibited a higher Ce:Zr ratio than the $Ce_{0.5}Zr_{0.5}O_2$. One could rationalize this difference proposing that in the latter the formation of the solid solution occurred to a greater extent than in the former.

In parallel with the changes observed in the crystalline phases by the addition of Ce, significant differences in specific surface area were observed for the Ce-promoted catalysts in comparison with the unpromoted ZrO_2. For example, while the BET area of ZrO_2 was only $35\,m^2/g$, that of the $Ce_{0.5}Zr_{0.5}O_2$ was $90\,m^2/g$.

The reducibility of the support is a very important issue in connection with its ability to generate oxygen vacancies and to transfer the oxygen onto the metal particle [21]. The pulse studies mentioned above [17] demonstrated that, when using ZrO_2 as a support in the absence of Ce, the presence of the oxygen vacancies is a requisite for the dissociation of CO_2. More recently, we have shown that when CO_2 pulses are sent over the Pt/ZrO_2 catalyst, no dissociation occurs, but if it is sent after a series of CH_4 pulses, which partially reduce the support, CO_2 is readily dissociated [21]. By addition of Ce, an enhancement of the oxygen exchange capacity occurs, improving the metal-cleaning ability. To find a correlation between the catalyst activity and the oxygen exchange capacity, it is important to determine the reducibility of the different Ce-promoted catalysts. To do this, we have employed XPS.

Fig. 2 shows XPS spectra in the binding energy region corresponding to Ce (3d) for the catalysts series. Each sample was first calcined, then reduced in H_2 at 773 K for 1 h, heated to 1073 K in He, and cooled to room temperature under He. Special precautions were taken to avoid any contact with air before introduction in the XPS analysis chamber (see section 2). It can be observed that each spectrum is composed by several components (eight as determined by least-squares fitting). The complexity of the photoelectron spectra observed in this region has been previously reported and has been rationalized in terms of a hybridization

Table 1
Surface atomic ratios as determined by XPS on the fresh catalysts reduced at 773 K and after 2 h reaction at 1073 K and a CH_4:CO_2 ratio of 2:1[a,b]

Sample	Ce/Zr ratio fresh samples	Ce/Zr ratio spent samples	Pt/(Ce+Zr) ratio fresh samples	Pt/(Ce+Zr) ratio spent samples	Metal fraction exposed (H:Pt)
Pt/ZrO_2	–	–	0.096	0.020	–
$Pt/Ce_{0.25}Zr_{0.75}O_2$	4.2	4.5	0.019	0.016	0.47
$Pt/Ce_{0.5}Zr_{0.5}O_2$	1.5	1.4	0.024	0.018	0.34
$Pt/Ce_{0.75}Zr_{0.25}O_2$	12.0	11.5	0.016	0.015	0.29
Pt/CeO_2	–	–	0.044	0.030	–

[a] Metal fraction exposed for the fresh catalysts reduced at 773 K calculated from hydrogen chemisorption.
[b] The XPS lines used to calculate the atomic ratios were Pt (4f), Zr (3d), and Ce (3d). Atomic sensitivity factors for these lines were those reported by Physical Electronics as empirically determined for the PHI 5800 XPS spectrometer.

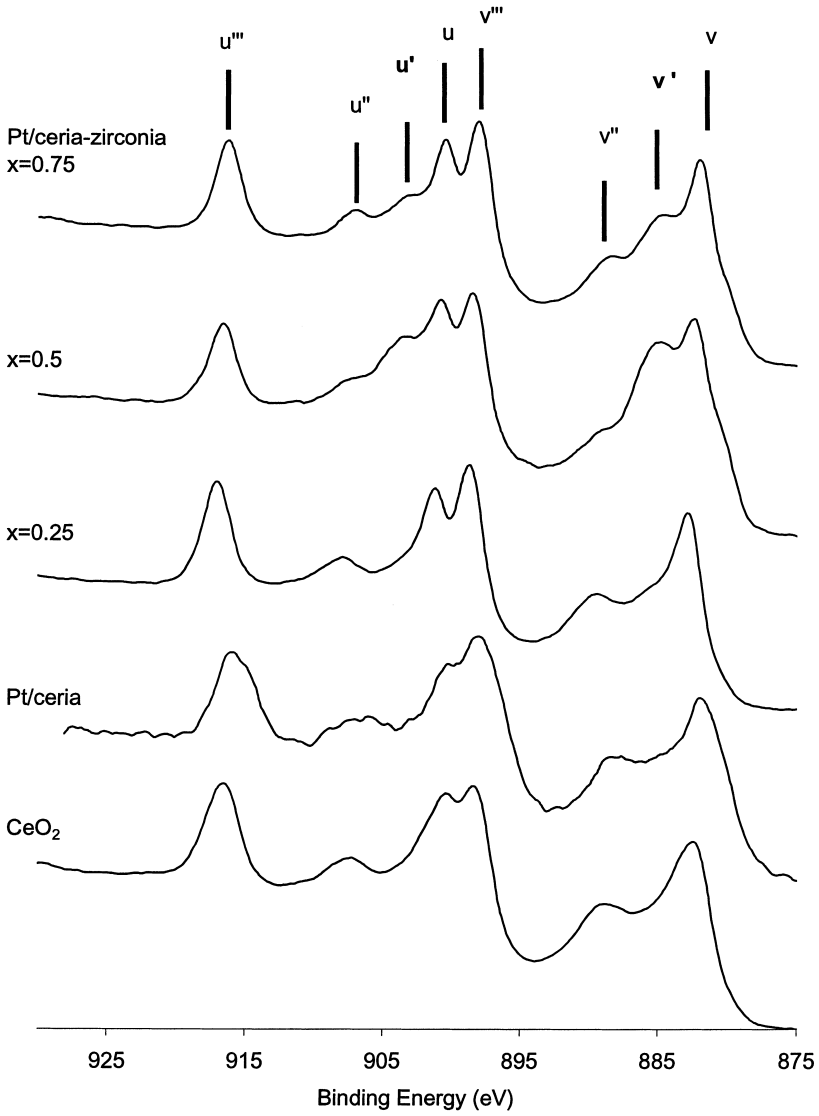

Fig. 2. Ce (3d) XPS spectra for CeO_2 and $Pt/Ce_xZr_{(1-x)}O_2$ catalysts.

between the partially occupied 4f levels in the Ce and the 2p states of oxygen [32,37]. Following the labeling first used by Burroughs et al. [38], the peaks labeled v correspond to Ce $3d_{5/2}$ contributions and those labeled u represent the Ce $3d_{3/2}$ contributions. The bands v, v″, and v‴(and those for u) are attributed to Ce^{4+}, while v′ and u′ are due to Ce^{3+}.

In line with this description, Fig. 2 shows that the peaks labeled u′ and v′ are more intense for the $Pt/Ce_xZr_{1-x}O_2$ catalysts in comparison with those for Pt/CeO_2 and CeO_2. In fact, in these last two samples, the peaks u′ and v′are practically absent. It is seen that the increase in v′ occurred at the expense of a decrease in v″. Clearly, among the $Pt/Ce_xZr_{1-x}O_2$ series the one that exhibits the greater v′:v″ and u′:u″ ratios is the one with composition $Ce_{0.5}Zr_{0.5}O_2$. To make a more quantitative comparison of the degree of Ce reduction, the u‴ peak is the most convenient feature since it does not overlap with the others. The measurement of the area under this u‴ peak relative to the total area under the Ce 3d spectra has been used in the past to calculate the fraction of Ce in the 4+ state [31,32,39]. The fractional areas of the u‴ peak in the total Ce (3d) region for the different catalysts investigated in this contribution are shown in Table 2. Reference values of compounds containing cerium only in the Ce^{4+} ($Ce(OH)_4$) and the Ce^{3+} ($CeAlO_3$ on Al_2O_3) oxidation states are included for comparison. The percent of Ce^{3+} in the samples estimated from the XPS data are also shown in Table 2. It is seen that the reducibility of the support is enhanced when the mixed solid is formed, and the percent of Ce^{3+} goes through a maximum when the composition is $Ce_{0.5}Zr_{0.5}O_2$.

Interestingly, Fornasiero et al. [40,35] in an investigation of Rh-loaded $Ce_xZr_{(1-x)}O_2$ with varying Ce/Zr ratios ($x = 0.1$–0.9) found that the reducibility of this series, as measured by the temperature required to reduce the

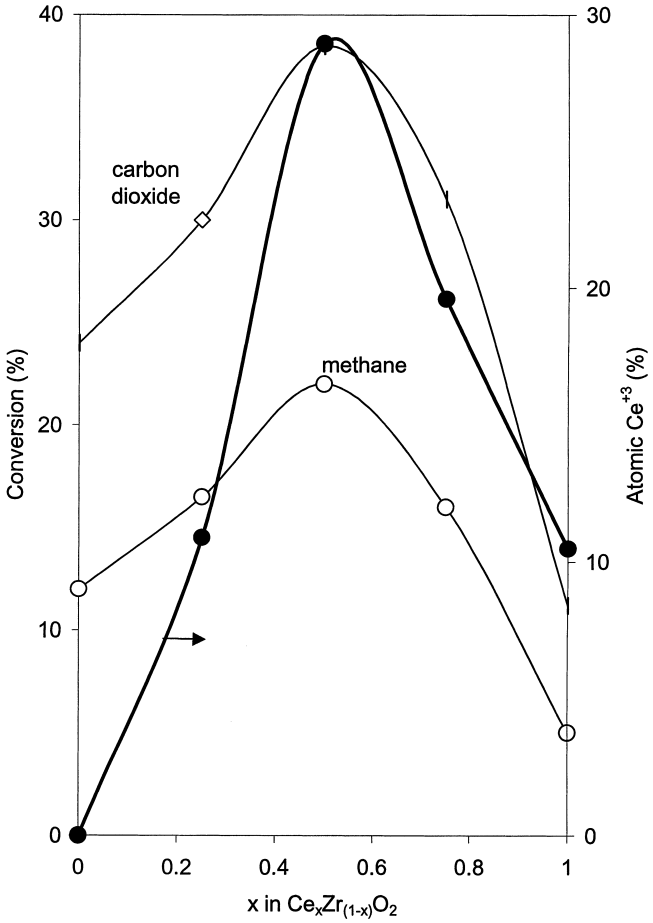

Fig. 3. Catalytic activity and reducibility of the support. CH_4 conversion (open circles) and CO_2 conversion (open diamonds) vs. fraction of Ce in the support (TOS = 22 h, T_{Rxn} = 1073 K and CH_4:CO_2 ratio=2:1). Atomic Ce^{3+} percent in $Ce_xZr_{1-x}O_2$ (full circles) vs. fraction of Ce in the support (XPS data recorded on the reduced sample).

oxide, strongly depended on the Ce/Zr ratio and it exhibited a maximum of reducibility (i.e. minimum temperature) for the composition $Ce_{0.5}Zr_{0.5}O_2$, in perfect agreement with the results reported in this work. They attributed the observed reducibility enhancement to an increased oxygen mobility in the bulk of the mixed oxide induced by the incorporation of Zr into the CeO_2 lattice. Similarly, Hori et al. [41] have recently observed that the rate of oxygen release in the presence of CO is twice as fast on Pt–ceria–zirconia than on Pt-pure ceria catalysts.

Table 2
Percent area of the XPS u‴ peak, calculated with respect to the total area of the Ce (3d) region[a]

Sample	u‴ in Ce(3d) (area %)	Atomic Ce^{3+} (%)	Reference
$Pt/Ce_{0.25}Zr_{0.75}O_2$	11.05	10.89	This work
$Pt/Ce_{0.5}Zr_{0.5}O_2$	8.81	28.95	This work
$Pt/Ce_{0.75}Zr_{0.25}O_2$	9.97	19.6	This work
Pt/CeO_2	11.1	10.48	This work
$Ce(OH)_4$	12.4	0	[31]
$CeAlO_3$:Al_2O_3	0	100	[31]

[a] This peak corresponds to the atomic percent of Ce^{4+} in the sample. The atomic percent of Ce^{3+} is obtained from the difference between total Ce and Ce^{4+}, taken the $Ce(OH)_4$ from [31] as a reference for 100% Ce^{4+}.

In accordance with our previous X-ray absorption observations [17] the XPS analysis of the Pt 4f peaks obtained on all reduced and spent samples of this series showed that Pt was in the metallic state. However, XAS is a bulk technique and at that time we could not rule out that a very thin oxidized layer covered the Pt particle and was not detected by the technique. However, XPS is a surface-sensitive technique and a surface oxide layer should be easily detected. Therefore, this result definitely demonstrates that partial oxidation of Pt does not occur during reaction.

3.2. Catalytic activity measurements

Several $Pt/Ce_xZr_{1-x}O_2$ catalysts were examined with different percentages of the Ce promoter. Of the three catalysts prepared by the co-precipitation method (Ce fraction: 0.25, 0.50 and 0.75) the $Pt/Ce_{0.5}Zr_{0.5}O_2$ catalyst proved to have significantly higher catalytic activity than either of the other two co-precipitated catalysts or the Pt/ZrO_2 and Pt/CeO_2. As shown in Fig. 3, the conversions of CH_4 and CO_2 after 22 h

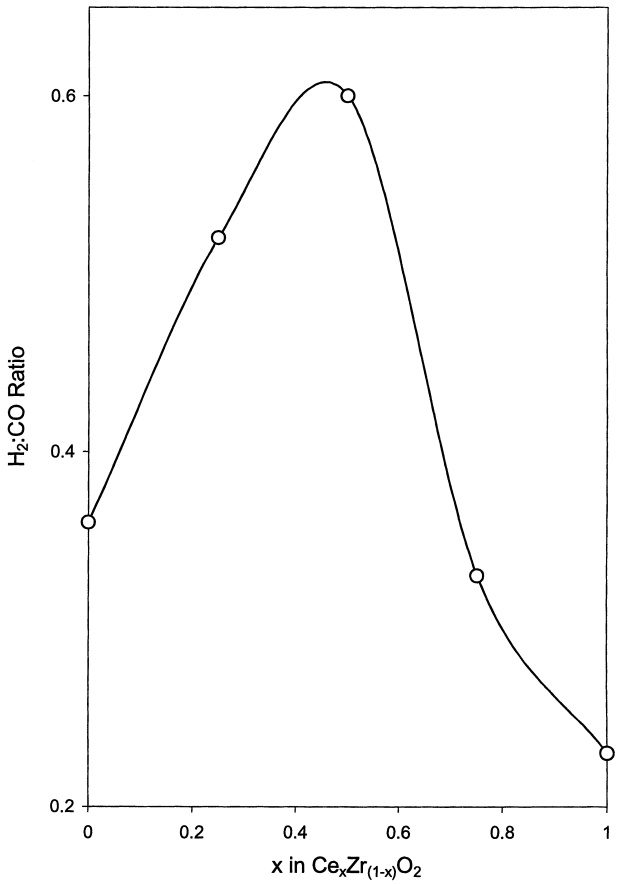

Fig. 4. H_2:CO ratio vs. fraction of Ce in the support for $Pt/Ce_xZr_{1-x}O_2$ catalysts (TOS = 22 h, T_{Rxn} = 1073 K and CH_4:CO_2 ratio=2:1).

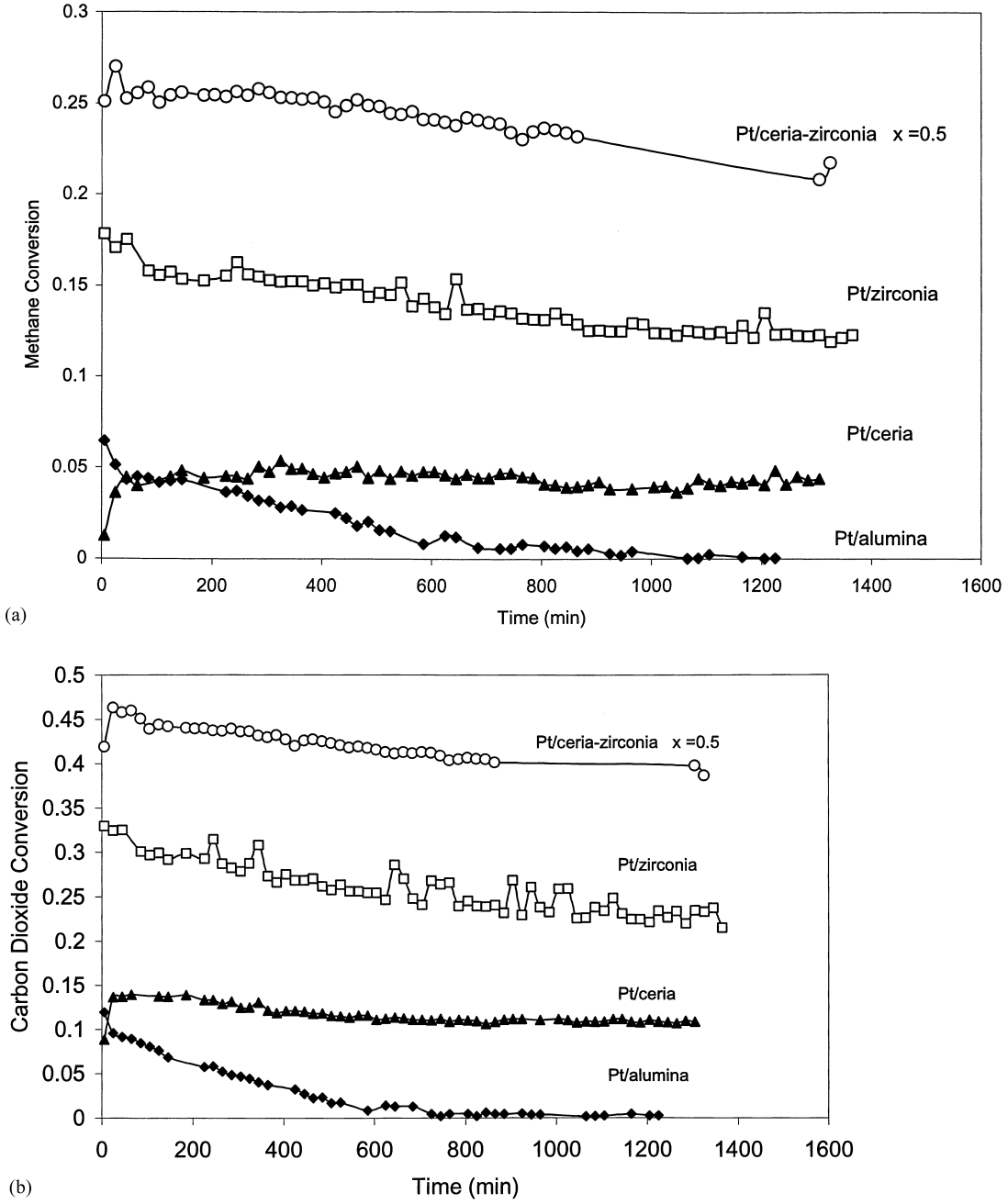

Fig. 5. Catalytic activity vs. time-on-stream for Pt/Al_2O_3, Pt/ZrO_2, Pt/CeO_2, and $Pt/Ce_{0.5}Zr_{0.5}O_2$ catalysts. Reaction conditions: TOS = 22 h, T_{Rxn} = 1073 K and CH_4:CO_2 ratio=2:1. (a) CH_4 fractional conversion. (b) CO_2 fractional conversion.

of reaction when plotted as a function of Ce% in the support go through a maximum at 50% Ce for the $Pt/Ce_{0.5}Zr_{0.5}O_2$ catalyst. It is important to compare this activity trend with the reducibility of the support as measured by XPS. When the fraction of reduced Ce (i.e. fraction of Ce^{3+}) in the support is plotted together with the activity pattern a striking relationship between activity and reducibility is clearly demonstrated. As illustrated in Fig. 4, the H_2/CO ratio obtained from the reaction data follows the same trend as the activity shown in Fig. 3. The H_2/CO ratio after 22 h of reaction is highest for the $Pt/Ce_{0.5}Zr_{0.5}O_2$ catalyst, but in all cases, it is lower than 1, due to a contribution of the reverse water gas shift reaction which converts H_2 and CO_2 to CO and water.

After the demonstration of the effect of the support reducibility on activity it is interesting to compare the stability displayed by catalysts with a reducible support such as Ce–ZrO_2 with one in which the support is non-reducible. Alumina is a good candidate for this comparison. Alumina has been extensively used for many industrial applications,

exhibiting a good thermal and chemical stability, in this case it may not be an appropriate support. For this comparison, a Pt/Al_2O_3 catalyst (1.5 wt.% Pt loading) was prepared and tested. As shown in Fig. 5a and b, the Pt/Al_2O_3 catalyst had a low initial activity and deactivated much more rapidly than the $Pt/Ce_{0.5}Zr_{0.5}O_2$ catalyst. The activity data for unpromoted Pt/ZrO_2 and Pt/CeO_2 catalysts have been also included in this figure. It can be observed that even the unpromoted Pt/ZrO_2 had much higher activity and stability than the one supported on alumina. The Pt/CeO_2 catalyst had an initial conversion comparable to that supported on alumina, however its stability was significantly better. The rapid deactivation of the Pt/Al_2O_3 catalyst can be attributed to coke deposition on the catalyst surface. The inability of the support to provide a high oxygen transfer and CO_2 dissociation makes the cleaning mechanism inoperative.

It is clear that the catalysts with ZrO_2, CeO_2, and Ce-promoted supports have better stability than the Al_2O_3 supported catalyst. However, the catalyst supported on unpromoted ZrO_2 also deactivates after some time. By comparison of the catalytic activity of the Pt/ZrO_2 catalyst and the Ce-promoted catalyst in Fig. 5, the importance of the promoter is evident as indicated by the improvement in activity. Even though the CeO_2 supported catalyst is relatively stable, the activity remains relatively low throughout the reaction. The relatively low activity of the CeO_2 catalyst can be attributed to a much lower surface area than zirconia.

3.3. Characterization of the spent catalysts and the carbon deposits after reaction

The fraction of metal exposed was determined by hydrogen chemisorption for the Pt catalysts supported on the double oxide supports. As summarized in Table 1, the fraction exposed after a reduction at 773 K is similar for the three samples. A more qualitative description of the fraction of metal exposed on the different catalysts before and after reaction can be obtained with XPS, by comparing the Pt/(Ce + Zr) atomic surface ratios. An increase in the Pt/(Ce + Zr) ratio indicates a higher fraction of the metal on the surface. Accordingly, the data in Table 1 indicates that the addition of Ce results in a decrease in the fraction of metal exposed for the catalysts reduced at 773 K. This decrease can be due to a larger metal particle size, or as has been observed before [42] to a partial coverage of the metal by CeO_x species, occurring during the high-temperature reduction. The interesting point is that after reaction, the metal fraction exposed is almost the same for all catalysts. Therefore, although particle size could have an important effect on the catalytic performance, they cannot play an important role in this catalyst series. Table 1 also shows the Ce/Zr ratios for the reduced and spent catalysts in the Ce–Zr series. An interesting trend appears. The catalyst containing $Ce_{0.25}Zr_{0.75}O_2$ shows a higher Ce/Zr ratio than that with composition $Ce_{0.5}Zr_{0.5}O_2$.

Table 3
Amount of carbon deposited on the different catalysts, as determined by TPO, using 5% O_2:He and a heating rate of 10 K/min, after 22 h reaction at 1073 K and a CH_4:CO_2 ratio of 2:1

Catalyst	Percent of carbon (wt.%)
Pt/ZrO_2	5.8
$Pt/Ce_{0.25}Zr_{0.75}O_2$	5.31
$Pt/Ce_{0.5}Zr_{0.5}O_2$	3.96
$Pt/Ce_{0.75}Zr_{0.25}O_2$	1.86
Pt/CeO_2	3.81
Pt/Al_2O_3	32.8

Table 3 summarizes the amount of carbon deposited on all the samples tested after 22 h of reaction at 1073 K and a CH_4:CO_2 ratio of 2:1. It is observed that the quantity of carbon deposited on the catalyst decreases as the ceria content increases. However, it appears that the amount of carbon deposited is not the most important parameter that relates to stability. In our previous paper [21] we found that although the unpromoted Pt/ZrO_2 catalyst and the 18 wt.% Ce-promoted catalyst formed in 22 h about the same amount of coke, the Ce-promoted catalyst was more active and stable. It is therefore, the ability of the catalyst to clean the active site what makes the catalyst active. It

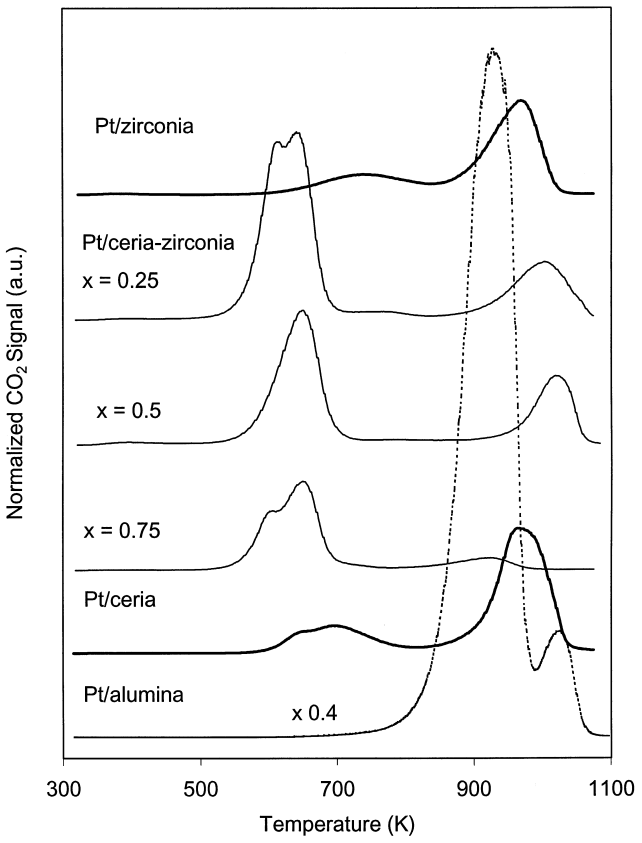

Fig. 6. Temperature programmed oxidation (5% O_2:He heating rate 10 K/min) for Pt/Al_2O_3, and $Pt/Ce_xZr_{(1-x)}O_2$ catalysts after exposure to a CH_4:CO_2=2:1 mixture at 1073 K for 22 h.

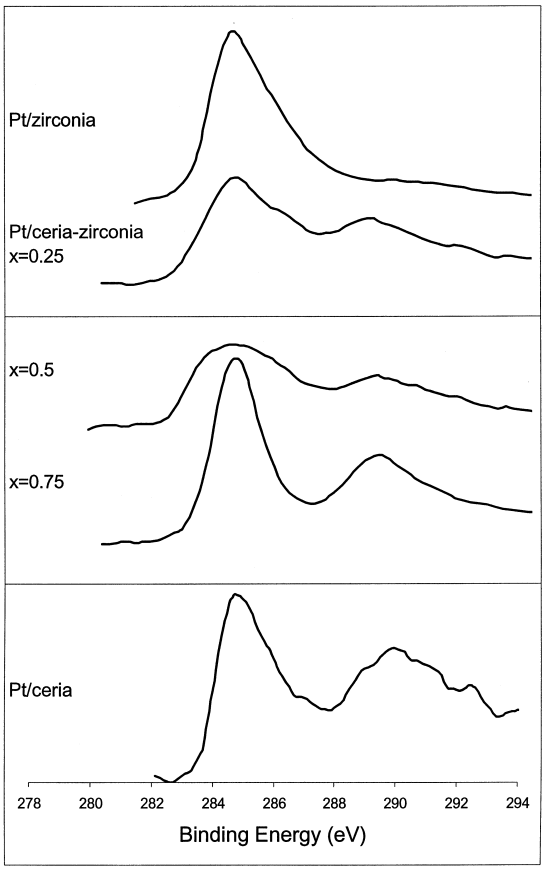

Fig. 7. C (1s) XPS spectra for $Pt/Ce_xZr_{(1-x)}O_2$ catalysts after exposure to a CH_4:CO_2=2:1 mixture at 1073 K for 2 h.

is possible that on the promoted catalyst, some carbon is deposited away from the metal–support interface, playing a minimal role in the deactivation.

To illustrate the ability of the promoted catalysts to eliminate coke more easily, Fig. 6 shows the TPO profiles for the six samples: Pt/ZrO_2, Pt/CeO_2, $Pt/Ce_xZr_{1-x}O_2$, and Pt/Al_2O_3 catalysts after 22 h of reaction at 1073 K and a CH_4:CO_2 feed ratio of 2:1. All the profiles showed two peaks, one in the low-temperature region, 623–723 K, and the other in the high-temperature region, 873–973 K. In agreement with results reported in our recent contribution [21] we observe that the peak in the high-temperature region is dominant in the unpromoted catalysts, while the peak at low temperature is more prominent in the $Pt/Ce_xZr_{1-x}O_2$ catalysts.

These two different oxidation regions can either be due to the presence of two different types of carbons or to a different location of the carbon on the surface of the catalyst. In the first case, the carbon that can be oxidized at lower temperatures would be more carbidic in nature or would contain a higher H:C ratio than the one oxidized at high temperatures, which should be more graphitic. If that were the case, one should observe differences in the binding energy of carbon as measured by XPS. Fig. 7 shows the XPS spectra in the C (1s) region for the five samples in the catalysts series after 2 h of reaction at 1073 K and a CH_4:CO_2 ratio of 2:1. To have an independent measurement of the carbon binding energies, they were aligned based on the Zr $4d_{5/2}$ line (182.4 eV) from the ZrO_2 support. After the short reaction time used for this particular set of samples, small amounts of carbon were present on the surface. Therefore, the different carbon species are more easily identifiable.

Table 4
Contributions to the C (1s) XPS spectra, determined by a least-squares fitting, expressed as atomic carbon percent[a]

Binding energy (eV)	Atomic carbon percent in $Pt/Ce_xZr_{(1-x)}O_2$				
	$x=0$	$x=0.25$	$x=0.5$	$x=0.75$	$x=1$
284–285	9.5	7.0	3.8	9.4	7.2
285–287	11.1	2.4	0.6	2.1	4.2
289–290	1.3	3.1	1.9	6.7	8.0

[a] XPS data obtained on the in $Pt/Ce_xZr_{(1-x)}O_2$ catalyst series after 2 h of reaction at 1073 K and a CH_4:CO_2 ratio of 2:1.

Three contributions can be identified in the spectra by least-squares fitting, one in the region 284–285 eV, a second one that appears as a shoulder of the first one around 285–287 eV, and a third contribution at around 288–290 eV. The first two regions are associated with coke deposits while the high-binding-energy region is due to carbonate species on the surface. Table 4 summarizes the contribution of each region to the total carbon content in the samples, as determined by the fitting. It is clear that the contribution of the high-binding-energy peak to the total carbon area increases with the amount of Ce in the sample, indicating that carbonate formation is favored in the presence of Ce. Bitter et al. [43] have noted that in general the oxides that are able to form carbonates (e.g. ZrO_2) promote the CO_2 reforming reaction more effectively than those that do not form carbonates (e.g. SiO_2). The formation of carbonates on the ceria-promoted catalysts qualitatively agrees with that observation. However, while the surface carbonate concentration continuously increases with Ce content, the activity goes through a maximum at an intermediate Ce concentration. Therefore, the reducibility, or rather the oxygen storage capacity, is the parameter that best correlates with activity (see Fig. 3).

The carbonaceous deposits on the $Pt/Ce_{0.5}Zr_{0.5}O_2$ catalyst after 22 h on stream at 1073 K and a CH_4:CO_2 ratio of 2:1 were also analyzed by XPS. Table 5 summarizes the atomic surface concentrations of carbon (as measured by XPS) on each of the binding energy regions. It is observed that after 22 h, both the contribution at 284–285 eV and that at 285–287 eV become of the same order. Moreover, a partial TPO was conducted stopping the heating at 723 K and then cooling down in He. This partial TPO was an attempt to see if the fraction of carbon that gets oxidized in the low temperature region of the TPO (see Fig. 6) was chemically distinguishable from that oxidized at high temperatures. However, the decrease in carbon concentration after this

Table 5
Contributions to the C (1s) XPS spectra determined by least-squares fitting and expressed as atomic carbon percent[a]

Binding energy (eV)	Surface atomic carbon percent in $Pt/Ce_{0.5}Zr_{0.5}O_2$			
	TOS = 2 h	TOS = 22 h	TOS = 22 h TPO up to 723 K	TOS = 22 h TPO up to 1073 K
284–285	0.85	9.58	4.63	0.15
285–287	3.53	10.70	4.34	4.30
289–290	1.95	4.0	1.99	0.98

[a] XPS data taken on the $Pt/Ce_{0.5}Zr_{0.5}O_2$ catalyst after reaction at 1073 K and a CH_4:CO_2 ratio of 2:1. Time-on-stream (TOS) = 2 and 22 h. Also included are data obtained after TPO up to 723 and 1073 K, respectively.

partial TPO was about 50% for all three types of carbon. Therefore, it appears that the different peaks that we observe in TPO are not due to different forms of carbon, but rather to different locations on the catalyst surface.

It is well known that the oxidation of carbon, occurring in TPO, is catalyzed by the metal on the sample. Therefore, those carbon deposits left near the metallic particle will be more easily oxidized. At the same time, it is interesting to note that on the promoted $Pt/Ce_xZr_{1-x}O_2$ catalysts, most of the carbon was oxidized at the low-temperature region. This could certainly be ascribed to the higher oxygen exchange capacity of Ce, which can have an important effect in catalyzing the oxidation during the TPO by transferring oxygen atoms across the surface onto the carbon deposits. The low-temperature peaks observed in TPOs of coked Pt/Al_2O_3 catalysts have been typically ascribed to carbon near the metal particles, while those at high temperatures have been ascribed to carbon on the support [44]. However, in the case of $Pt/Ce–ZrO_2$ catalysts we ascribe this low-temperature TPO peak to carbon that is not immediately near the metal particle, since as indicated by the lack of catalyst deactivation, this carbon is continuously eliminated during reaction. Therefore, we can conclude that on the Ce-promoted catalysts the immediate proximity of the metal–support interface is kept free of coke all the time, as the absence of any deactivation demonstrates. There is a region near the particles, but not exactly at the interface, which may accumulate small amounts of carbon.

The clear activity enhancement caused by the addition of Ce to zirconia is certainly related to the ability of Ce to accelerate the oxygen exchange capacity. As we mentioned above, a higher rate of oxygen transfer helps to keep the metal surface free of carbon. However, if one compares the long-term stability of the zirconia-supported catalyst with that of the ceria–zirconia-supported catalysts, there is no much difference (see Fig. 5). It is the activity level that is higher in the promoted catalyst. We explain this enhancement in activity by the two-path mechanism proposed before [3,7,16,17]. During the first moments in contact with the catalyst, the reacting mixture reaches a balance resulting from the methane decomposition and the oxygen transfer. If the oxygen transfer is fast enough to keep up with the methane decomposition on the metal, the activity stabilizes at a high rate. This is the case observed here for the catalysts supported on ceria–zirconia. If the oxygen transfer lags behind, carbon deposition occurs as a result of the initially rapid methane decomposition. This carbon deposition slows down the rate of methane decomposition until a balance is reached with the rate of oxygen transfer. This is the situation that takes place on the zirconia-supported catalyst. Finally, when the oxygen transfer is much slower, the carbon deposition cannot be controlled and the catalyst rapidly deactivates, as it is observed for the alumina- or silica-supported catalysts.

4. Conclusions

The main conclusions of the present study can be summarized as follows:

1. The catalytic activity of Pt/ZrO_2 is greatly enhanced by the addition of Ce to the support. The activity goes through a maximum at a composition $Pt/Ce_{0.5}Zr_{0.5}O_2$.
2. The reducibility, and, therefore, the oxygen exchange capacity, of the support also has a maximum at the composition $Ce_{0.5}Zr_{0.5}O_2$.
3. The excellent correlation between support reducibility and catalytic activity gives further support to the two-path mechanism for the CO_2 reforming of methane proposed before. Accordingly, methane decomposes on the metal surface, producing hydrogen and carbon that then reacts with oxygen from the support, which is continuously replenished by the dissociation of CO_2. With the presence of an oxide such as ceria, which greatly enhances the rate of oxygen transfer, this step is accelerated.

Acknowledgements

This work was supported by the DoE/EPSCOR program of the Department of Energy (DE-FG02-99ER45759). We acknowledge the International Division of the National Science Foundation for partial support and the NATO Science Program for a collaborative research grant (CRG No. 971062). One of us (R.R.S.) is especially indebted to CNPQ (Brazil) for financial support. We acknowledge Carla E. Hori for the preparation of the $Ce_xZr_{1-x}O_2$ samples.

References

[1] A. Erdohelyi, J. Cserenyi, F. Solymosi, J. Catal. 141 (1993) 287.
[2] M. Bradford, M.A. Vannice, Catal. Lett. 48 (1997) 31.

[3] M. Bradford, M.A. Vannice, J. Catal. 173 (1998) 157.
[4] A.M. Gadalla, M.E. Sommer, Chem. Eng. Sci. 44 (1989) 2825.
[5] D. Qin, J. Lapszewicz, Catal. Today 21 (1994) 551.
[6] X. Xiaoding, J.A. Moulijn, Energy and Fuels 10 (1996) 305.
[7] J.R.H. Ross, A.N.J. van Keulen, M.E.S. Hegarty, K. Seshan, Catal. Today 30 (1996) 193.
[8] S.B. Wang, G.Q. Lu, Energy and Fuels 10 (1996) 896.
[9] F. Solymosi, G. Kustan, A. Erdohelyi, Catal. Lett. 11 (1991) 149.
[10] V.R. Choudhary, A.M. Rajput, Ind. Eng. Chem. Res. 35 (1996) 3934.
[11] A. Takano, T. Tagawa, S. Goto, J. Chem. Eng. Jpn. 27 (1994) 727.
[12] S. Teuner, Hydroc. Proc. 64 (1985) 106.
[13] M.E.S. Hegarty, J.R.H. Ross, A.M. O'Connor, Catal. Today 42 (1998) 225.
[14] P. Gronchi, C. Mazzocchia, E. Tempesti, R. Del Rosso, in: Centi et al. (Eds.), Environmental Catalysis, SCI Publishers, Rome, 1995, p. 627.
[15] K. Seshan, J.R.H. Ross, P.D. Mercera, E. Xue, German Patent DE 9400513 (1994).
[16] J.H. Bitter, W. Hally, K. Seshan, J.G. van Ommen, J.A. Lercher, Catal. Today 29 (1996) 732.
[17] S.M. Stagg, E. Romeo, C. Padro, D.E. Resasco, J. Catal. 178 (1998) 139.
[18] L. Tournayan, A. Auroux, H. Charcosset, R. Szymanski, Ads. Sci. Tech. 2 (1985) 55.
[19] S.M. Stagg, D.E. Resasco, Stud. Surf. Sci. Catal. 119 (1998) 813.
[20] S.M. Stagg-Williams, R. Soares, E. Romero, W.E. Alvarez, D.E. Resasco, Stud. Surf. Sci. Catal. 130 (2000) 3663.
[21] S. M Stagg-Williams, F.B. Noronha, G. Fendley, D.E. Resasco, J. Catal. 194 (2000) 240.
[22] A.M. Efstathiou, A. Kladi, V.A. Tsipouriari, X.E. Verykios, J. Catal. 158 (1996) 64.
[23] A. Trovarelli, C. de Leitenmburg, G. Dolcetti, Chemtech 27 (1997) 32.
[24] M.H. Yao, R.J. Baird, F.W. Kunz, T.E. Hoost, J. Catal. 166 (1997) 67.
[25] P.J. Schmitz, R.K. Usmen, C.R. Peters, G.W. Graham, R.W. McCabe, Appl. Surf. Sci. 72 (1993) 181.
[26] H. Cordatos, T. Bunluesin, J. Stubenrauch, J.N. Vohs, R.J. Gorte, J. Phys. Chem. 100 (1996) 785.
[27] E.S. Putna, T. Bunluesin, X.L. Fang, R.J. Gorte, J.N. Vohs, R.E. Lakis, T. Egami, Catal. Today 50 (1999) 343.
[28] G.S. Zafiris, R.J. Gorte, J. Catal. 139 (1993) 561.
[29] G.S. Zafiris, R.J. Gorte, J. Catal. 143 (1993) 86.
[30] C.E. Hori, H. Permana, K.Y. Simon Ng, A. Brenner, K. More, K.M. Rahmoeller, D. Belton, Appl. Catal. B 16 (1998) 105.
[31] J.Z. Shyu, W.H. Weber, H.S. Gandhi, J. Phys. Chem. 92 (1988) 4964.
[32] J.Z. Shyu, K. Otto, W.L.H. Watkins, G.W. Graham, R.K. Belitz, H.S. Gandhi, J. Catal. 114 (1988) 23.
[33] P.D.L. Mercera, J.G. Van Ommen, E.B.M. Doesburg, A.J. Burgraaf, J.R.H. Ross, Appl. Catal. 57 (1990) 127.
[34] P. Turlier, J.A. Dalmon, G.A. Martin, P. Vergnon, Appl. Catal. 29 (1987) 305.
[35] G. Vlaic, P. Fornasiero, S. Geremia, J. Kaspar, M. Graziani, J. Catal. 168 (1997) 386.
[36] G. Colón, M. Pijolat, F. Valdivieso, J. Kaspar, E. Finocchio, M. Daturi, C. Binet, J.C. Lavalley, R.T. Baker, S. Bernal, J. Chem. Soc., Faraday Trans. 94 (1998) 3717.
[37] F. Le Normand, J. El Fallah, L. Hilaire, P. Legare, A. Kotani, J.C. Parlebas, Solid State Commun. 71 (1989) 885.
[38] P. Burroughs, A. Hammett, A.F. Orchard, G. Thornton, J. Chem. Soc., Dalton Trans. 17 (1976) 1686.
[39] K. Bak, L. Hilaire, Appl. Surf. Sci. 70 191 (1993).
[40] P. Fornasiero, R. Di Monte, G. Ranga Rao, J. Kaspar, S. Meriani, A. Trovarelli, M. Graziani, J. Catal. 151 (1995) 168.
[41] C.E. Hori, A. Brenner, K.Y. Simon Ng, K.M. Rahmoeller, D. Belton, Catal. Today 50 (1999) 299.
[42] G.L. Haller, D.E. Resasco, Adv. Catal. 36 (1989) 173.
[43] J.H. Bitter, K. Seshan, J.A. Lercher, J. Catal. 171, 279 (1997).
[44] R. Bacaud, H. Charcosset, M. Guemin, H. Torresea-Hidalgo, L. Tournayan, Appl. Catal. 1 (1981) 81.